Journal of Computational and Applied Mathematics 372 (2020) 112719

Contents lists available at ScienceDirect

Journal of Computational and Applied Mathematics

journal homepage: www.elsevier.com/locate/cam

Error analysis of full-discrete invariant energy quadratization schemes for the Cahn–Hilliard type equation

Jun Zhang [a,b], Jia Zhao [c,*], Yuezheng Gong [d]

[a] Guizhou Key Laboratory of Big Data Statistics Analysis, Guizhou University of Finance and Economics, Guiyang, Guizhou, 550025, China
[b] Computational Mathematics Research Center, Guizhou University of Finance and Economics, Guiyang, Guizhou 550025, China
[c] Department of Mathematics and Statistics, Utah State University, Logan, UT, 84322, USA
[d] College of Science, Nanjing University of Aeronautics and Astronautics, Nanjing 210016, China

ARTICLE INFO

Article history:
Received 7 February 2019
Received in revised form 9 July 2019

Keywords:
Cahn–Hilliard equation
Invariant energy quadratization
Unconditionally energy stable
Error estimate

ABSTRACT

In this paper, we present the error analysis for a fully discrete scheme of the Cahn–Hilliard type equation, along with numerical verifications. The numerical schedule is developed by first transforming the Cahn–Hilliard type equation into an equivalent form using the invariant energy quadratization (IEQ) technique. Then the equivalent form is discretized by using the linear-implicit Crank–Nicolson method for the time variable and the Fourier pseudo-spectral method for the spatial variables. The resulted full-discrete scheme is linear and unconditionally energy stable, which makes it easy to implement. By constructing an appropriate interpolation equation, the uniform boundedness of the numerical solution is obtained theoretically. Then, we prove that the numerical solutions converge with the order $\mathcal{O}((\delta t)^2 + h^m)$, where δt is the temporal step and h is the spatial step with m the regularity of the exact solution. Several numerical examples are presented to confirm the theoretical results and demonstrate the effectiveness of the presented linear scheme. The numerical strategies and analytical tools in this paper could be readily applied to study other phase field models or gradient flow problems.

1. Introduction

The Cahn–Hilliard (CH) equation was originally proposed by Cahn and Hilliard [1] to describe the process of coarsening dynamics and phase separation. Nowadays, the CH model has emerged as a classical mathematical physics model in various applications, including multiphase fluid flows, polymer physics, soft matter (cf. [2–7]). Thus, it is imperative to propose some accurate and efficient numerical methods to solve the CH equation. An important feature of the equation is that it satisfies an energy dissipation law. It is natural to develop efficient numerical methods that preserve the energy dissipation law in the discrete level. Such numerical schemes are known as energy-stable schemes or structure-preserving schemes. If the scheme does not have any time step restriction to preserve the energy-dissipation property, the schemes are called unconditionally energy stable. The difficulty of developing such schemes lies in the discretization of nonlinear terms in the CH equation. Also, if we treat all the nonlinear terms implicitly, it will generate a nonlinear system for each time step, and the computational is very large. But, if we treat all the nonlinear terms explicitly, it will lead to serious time step constraints and the scheme does not satisfy the energy dissipation property in most cases.

* Corresponding author.
E-mail addresses: zj654440@163.com (J. Zhang), jia.zhao@usu.edu (J. Zhao), gongyuezheng@nuaa.edu.cn (Y. Gong).

https://doi.org/10.1016/j.cam.2020.112719
0377-0427/

Over the past few decades, many researchers are committed to developing energy-stable schemes to solve the CH equation. In general, it is an active field for developing energy stable schemes for thermodynamically consistent models At present, the commonly used methods include the convex splitting approach [8–14], the stabilized approach [15–21], and many others [22–31]. The advantage of the convex splitting approach is that it is unconditional energy stable and uniquely solvable, by splitting the nonlinear terms into convex and concave parts and treating them differently. But, some nonlinear systems will be produced, which makes the calculation quite tricky, especially for long-term numerical simulation. The stabilized approach is simple and easy to apply, and only the constant-coefficient equations need to be solved for each time step. In the stabilized approach, the nonlinear function is treated full-explicitly. To obtain energy stability results, one has to add a stable term to balance the influence of explicit terms. However, this method is conditionally energy stable, and it has a restriction potential functionals. To weaken this restriction, Li, Qiao, and Tang [32,33] constructed a new stabilization method, but it is still conditionally stable. Based on the Lagrange multiplier method [22,34], Yang et al. [35–40] proposed the IEQ method. The key idea of this method is to transform the original nonlinear potential function into a quadratic form by introducing two new variables. The advantages of this method are linear and unconditionally stable. Meanwhile, this method can be extended to higher-order methods [41]. It is necessary to assume that the double-well potential $F(x)$ is bounded from below, besides, due to the special construction of quadratic functions, it involves solving complicated variable coefficient equations. Shen et al. [31] made appropriate modifications to quadratic functions and proposed the scalar auxiliary variable (SAV) approach, which is also linear, and unconditional energy stable. Besides, this method has the advantage that only the constant-coefficient equations need to be solved.

Rigorous error estimates have been carried out for the SAV approach [42], and the first-order semi-discrete IEQ approach [38]. Unfortunately, results on the error estimate of the fully discrete and second-order IEQ schemes for solving the Cahn–Hilliard type equations are still missing. The nonlinear quadratic term introduced by the IEQ method brings considerable trouble to error analysis of the full-discrete scheme. In this article, we propose a fully discrete linear scheme for the CH type equation, where we use the Crank–Nicolson method for time discretization and the Fourier pseudo-spectral method for the spatial discretization. Rigorous convergence analysis is provided for this full-discrete scheme. Specifically, through our special construction, the projection of the exact solution on Fourier space satisfies an optimal regularity requirement. Then, under appropriate assumptions, we prove that the numerical method leads to second-order accuracy in the time direction and spectral accuracy in the space direction. Afterward, some numerical examples are conducted to support the theoretical claims.

The rest of the article is structured as follows. In Section 2, we present the fully discrete scheme. Then, we prove that the fully discrete scheme is unconditionally energy stable and unique solvable in Section 3. Afterward, in Section 4, we present our proofs showing that the fully discrete scheme is second order convergent in time and spectral convergent in space. In Section 5, several numerical experiments are performed to verify our theoretical results. The conclusion of this article is given in the last section.

2. Full discrete numerical scheme

In this paper, we consider the following general energy functional

$$E(\phi)=\int_{\Omega}\Big(\frac{1}{2}|\nabla\phi|^2+F(\phi)\Big)dx, \tag{1}$$

where $F'(\phi)=f(\phi)$ is the nonlinear potential. Then, we can get the following Cahn–Hilliard type equation as

$$\begin{cases}\phi_t=\Delta w,\\ w=-\Delta\phi+F'(\phi).\end{cases} \tag{2}$$

2.1. Model reformulation using the invariant energy quadratization technique

To solve the Cahn–Hilliard type equation (2), we need to reformulate it into an equivalent form using the invariant energy quadratization technique. In details, we denote

$$q(\phi)=\sqrt{F(\phi)-\frac{\gamma}{2}\phi^2+B},\quad g(\phi)=2\frac{d}{d\phi}q(\phi)=\frac{f(\phi)-\gamma\phi}{\sqrt{F(\phi)-\frac{\gamma}{2}\phi^2+B}}, \tag{3}$$

where B be a constant such that $q(\phi)$ is well-defined. Then, we rewrite Eq. (2) as follows

$$\begin{cases}\phi_t=\Delta w,\\ w=-\Delta\phi+\gamma\phi+g(\phi)q,\\ q_t=\frac{1}{2}g(\phi)\phi_t,\end{cases} \tag{4}$$

subject to the consistent initial and boundary conditions

$$\phi|_{t=0}=\phi_0,\quad q|_{t=0}=\sqrt{F(\phi_0)-\frac{\gamma}{2}\phi_0^2+B}, \tag{5}$$

$$\phi,\ w \text{ are periodic.} \tag{6}$$

It could be easily verified that the transformed model (4) is equivalent to the original CH model (2), and they obey the same energy dissipation law. Actually, by taking the L^2 inner product of (4) with w, ϕ_t, $2q$, respectively, we have

$$\frac{d}{dt}E(\phi, q) = -\int_{\Omega} |\nabla w|^2 d\boldsymbol{x}, \tag{7}$$

where

$$E(\phi, q) = \int_{\Omega} \frac{1}{2}|\nabla\phi|^2 + \frac{\gamma}{2}\phi^2 + q^2 d\boldsymbol{x} - B|\Omega|. \tag{8}$$

Note that the energy $E(\phi, q)$ is equivalent to $E(\phi)$ by acknowledging (3).

2.2. The fully discrete scheme

Before we present the fully discrete scheme, we introduce some notations that will be used frequently in the rest of this paper. Given $f(x, y) \in L^2(\Omega)$ with $\Omega = (0, L)^2$, its Fourier transform is denoted as

$$f(x, y) = \sum_{j,k=-\infty}^{\infty} \widehat{f}_{j,k} e^{\frac{2\pi}{L} i(jx+ky)}, \tag{9}$$

where the inverse transform is given as

$$\widehat{f}_{j,k} = \frac{1}{L^2}\int_{\Omega} f(x, y) e^{-\frac{2\pi}{L} i(jx+ky)} dxdy. \tag{10}$$

The truncated series is the projection onto the space S^N of trigonometric polynomials in x, y of degree up to N, given by

$$\mathcal{P}_N f(x, y) = \sum_{j,k=-N}^{N} \widehat{f}_{j,k} e^{\frac{2\pi}{L} i(jx+ky)}. \tag{11}$$

To obtain a pseudospectral approximation at a given set of points, an interpolation operator $\mathcal{I}_N$ is introduced. The Fourier interpolation of the function is defined by

$$(\mathcal{I}_N f)(x, y) = \sum_{j,k=-N}^{N} (\widehat{f_N})_{j,k} e^{\frac{2\pi}{L} i(jx+ky)}, \tag{12}$$

where $(\widehat{f_N})_{j,k}$ are computed based on the interpolation condition $f(x_j, y_k) = (\mathcal{I}_N f)(x_i, y_k)$ on the $(2N + 1) \times (2N + 1)$ equidistant points. In practice, one may compute the collocation coefficients $(\widehat{f_N})_{j,k}$ via FFT. The convergence of the derivatives of the projection and interpolation is given by

$$\|\partial^l f(x, y) - \partial^l \mathcal{P}_N f(x, y)\|_{L^2} \leq Ch^{k-l}\|f\|_{H^k}, \quad \text{for } 0 \leq l \leq k, \tag{13}$$

$$\|\partial^l f(x, y) - \partial^l \mathcal{I}_N f(x, y)\|_{L^2} \leq Ch^{k-l}\|f\|_{H^k}, \quad \text{for } 0 \leq l \leq k, k > \frac{d}{2}. \tag{14}$$

Note that C is a general constant in this paper (that is independent of temporal and spatial steps), but representing different values in different places. Given any real grid functions $\boldsymbol{f}$ and $\boldsymbol{g}$ (over the numerical grid), we introduce the following discrete L^2 norm and inner product

$$\|\boldsymbol{f}\|_2^2 = \langle \boldsymbol{f}, \boldsymbol{f}\rangle, \quad \langle \boldsymbol{f}, \boldsymbol{g}\rangle = \Big(\frac{L}{2N+1}\Big)^2 \sum_{j,k=0}^{2N} \boldsymbol{f}_{j,k}\boldsymbol{g}_{j,k}, \tag{15}$$

and the following property holds

$$\langle \boldsymbol{f}, D_N^2 \boldsymbol{g}\rangle = -\langle D_N \boldsymbol{f}, D_N \boldsymbol{g}\rangle, \tag{16}$$

where D_N denotes the discrete differentiation operator.

With all the notations above, we now present the following full-discrete scheme

$$\begin{cases} \frac{\phi^{n+1}-\phi^n}{\delta t} = D_N^2 \frac{w^{n+1}+w^n}{2}, \\ \frac{w^{n+1}+w^n}{2} = -D_N^2 \frac{\phi^{n+1}+\phi^n}{2} + \gamma \frac{\phi^{n+1}+\phi^n}{2} + g(\phi^*)\frac{q^{n+1}+q^n}{2}, \\ \frac{q^{n+1}-q^n}{\delta t} = \frac{1}{2} g(\phi^*)\frac{\phi^{n+1}-\phi^n}{\delta t}, \end{cases} \tag{17}$$

where $\phi^* = \frac{3}{2}\phi^n - \frac{1}{2}\phi^{n-1}$, $n \geq 1$, with $\phi^* = \phi^0$ for $n = 0$, and g is defined in (3).

2.3. Stability and uniqueness for the full-discrete scheme

First of all, we have the following energy stability results for the full-discrete scheme (17).

Lemma 2.1. *The full-discrete scheme (17) is unconditionally energy stable. And it follows the energy dissipation law as*

$$E(\phi^{n+1}, q^{n+1}) + \delta t \|D_N(\frac{w^{n+1}+w^n}{2})\|_2^2 = E(\phi^n, q^n), \tag{18}$$

and in particular $E(\phi^{n+1}, q^{n+1}) \le E(\phi^n, q^n)$, *with*

$$E(\phi^n, q^n) = \frac{1}{2}\|D_N\phi^n\|_2^2 + \frac{1}{2}\gamma\|\phi^n\|_2^2 + \|q^n\|_2^2 - B|\Omega|.$$

Proof. Taking the L^2 inner product of the first equation in (17) with $\delta t(w^{n+1}+w^n)$, and using integration by parts, we obtain

$$\left\langle \phi^{n+1}-\phi^n, w^{n+1}+w^n \right\rangle = -2\delta t\|D_N(\frac{w^{n+1}+w^n}{2})\|_2^2. \tag{19}$$

Taking the L^2 inner product of the second equation in (17) with $2(\phi^{n+1}-\phi^n)$, we obtain

$$\begin{aligned}\left\langle w^{n+1}+w^n, \phi^{n+1}-\phi^n \right\rangle =& \|D_N\phi^{n+1}\|_2^2 - \|D_N\phi^n\|_2^2 + \gamma(\|\phi^{n+1}\|_2^2 - \|\phi^n\|_2^2) \\ &+ \left\langle g(\phi^*)(q^{n+1}+q^n), \phi^{n+1}-\phi^n \right\rangle.\end{aligned} \tag{20}$$

Computing the L^2 inner product of the third equation in (17) with $2\delta t(q^{n+1}+q^n)$, we obtain

$$2\|q^{n+1}\|_2^2 - 2\|q^n\|_2^2 = \left\langle g(\phi^*)(\phi^{n+1}-\phi^n), q^{n+1}+q^n \right\rangle. \tag{21}$$

Summing above equation up and dividing both sides by 2, we have

$$\frac{1}{2}\|D_N\phi^{n+1}\|_2^2 - \frac{1}{2}\|D_N\phi^n\|_2^2 + \frac{1}{2}\gamma(\|\phi^{n+1}\|_2^2 - \|\phi^n\|_2^2) + \|q^{n+1}\|_2^2 - 2\|q^n\|_2^2 = -\delta t\|D_N(\frac{w^{n+1}+w^n}{2})\|_2^2.$$

Then we derive (18). This completes the proof.

Theorem 2.2. *The full-discrete scheme (17) is uniquely solvable.*

Proof. First, from the third equation of (17), we find

$$q^{n+1} = q^n + \frac{1}{2}g(\phi^*)(\phi^{n+1}-\phi^n). \tag{22}$$

Then, we can rewrite (17) as follows

$$\begin{cases}\phi^{n+1} - \frac{\delta t}{2}D_N^2 w^{n+1} = \xi_1, \\ P(\phi^{n+1}) - w^{n+1} = \xi_2,\end{cases} \tag{23}$$

where

$$\begin{cases}\xi_1 = \phi^n + \frac{\delta t}{2}D_N w^n, \\ \xi_2 = D_N^2\phi^n - \gamma\phi^n + g(\phi^*)(\frac{1}{2}g(\phi^*)\phi^n - 2q^n) + w^n, \\ P(\phi) = -D_N^2\phi + \gamma\phi + \frac{1}{2}g(\phi^*)^2\phi.\end{cases} \tag{24}$$

In other words, (23) could be written as

$$\mathcal{L}\begin{bmatrix}\phi^{n+1}\\ w^{n+1}\end{bmatrix} = \begin{bmatrix}\zeta_2\\ \zeta_1\end{bmatrix}, \quad \mathcal{L} = \begin{bmatrix}-D_N^2 + \gamma + \frac{1}{2}g(\phi^*)^2 & -1\\ 1 & -\frac{\delta t}{2}D_N^2\end{bmatrix}. \tag{25}$$

Thus, we can solve (ϕ^{n+1}, w^{n+1}) directly from the linear algebra equation (25). To show there exists a unique solution for (25), we only need to should $\mathcal{L}X = 0$ only has solution $X = 0$, with $\mathcal{L}$ the stiffness matrix.

Notice the facts, when φ satisfies the periodic boundary condition, we have

$$\langle P(\phi), \varphi\rangle = \langle D_N\phi, D_N\varphi\rangle + \gamma\langle\phi, \varphi\rangle + \frac{1}{2}\langle(g^*)^2\phi, \varphi\rangle = \langle\phi, P(\varphi)\rangle. \tag{26}$$

Then, the linear operator $P(\phi)$ is symmetric. Furthermore, we find

$$\langle P(\phi), \phi\rangle = \|D_N\phi\|_2^2 + \gamma\|\phi\|_2^2 + \frac{1}{2}\|g(\phi^*)\phi\|_2^2. \tag{27}$$

Thus the operator $P(\phi)$ is positive. Taking the inner product of the first equation in (17) with 1, we derive

$$\langle \phi^{n+1}, 1\rangle = \langle \phi^n, 1\rangle = \cdots = \langle \phi^0, 1\rangle. \tag{28}$$

Set $v_\phi = \frac{1}{|\Omega|}\langle \phi^0, 1\rangle$, $v_w = \frac{1}{|\Omega|}\langle w^{n+1}, 1\rangle$, and denote

$$\widehat{\phi}^{n+1} = \phi^{n+1} - v_\phi, \quad \widehat{w}^{n+1} = w^{n+1} - v_w. \tag{29}$$

Combining with (23), we know that $(\widehat{\phi}^{n+1}, \widehat{w}^{n+1})$ is the solution of the following equations

$$\begin{cases} \langle P(\phi), \psi\rangle - \langle w, \psi\rangle = \langle \xi_3, \psi\rangle, \\ \langle \phi, \varphi\rangle + \frac{\delta t}{2}\langle D_N w, D_N \varphi\rangle = \langle \xi_4, \varphi\rangle. \end{cases} \tag{30}$$

We denote the above system as follows

$$\langle \mathcal{L}X, Y\rangle = \langle \mathcal{F}, Y\rangle, \tag{31}$$

with $X = [\phi, w]^T$, $Y = [\varphi, \psi]^T$, $\mathcal{F} = [\xi_3, \xi_4]^T$. Thus, we find

$$\langle \mathcal{L}X, X\rangle = \frac{\delta t}{2}\|D_N w\|_2^2 + \langle P(\phi), \phi\rangle \tag{32}$$

Apparently, when $\mathcal{L}X = 0$, it holds $\langle \mathcal{L}X, X\rangle = 0$, then we can deduce that $X = 0$. Thus the linear system (31) is uniquely solvable. □

3. Convergence analysis

We denote Φ_N as the projection of ϕ into S^N, i.e.

$$\Phi_N(\cdot, t) = \mathcal{P}_N\phi(\cdot, t), \quad W_N(\cdot, t) = \mathcal{P}_N w(\cdot, t), \quad Q_N(\cdot, t) = \mathcal{P}_N q(\cdot, t). \tag{33}$$

It is easy to find that

$$\frac{\partial}{\partial t}\Phi_N = \frac{\partial}{\partial t}\mathcal{P}_N\phi = \mathcal{P}_N\frac{\partial}{\partial t}\phi, \quad \frac{\partial}{\partial t}Q_N = \frac{\partial}{\partial t}\mathcal{P}_N q = \mathcal{P}_N\frac{\partial}{\partial t}q. \tag{34}$$

We rewrite Eq. (4) as follows

$$\begin{cases} \partial_t\Phi_N = \Delta W_N + r_1, \\ W_N = -\Delta\Phi_N + \gamma\Phi_N + g(\Phi_N)Q_N + r_2, \\ \partial_t Q_N = \frac{1}{2}g(\Phi_N)\partial_t\Phi_N + r_3, \end{cases} \tag{35}$$

where

$$\begin{cases} r_1 = (\partial_t\Phi_N - \partial_t\phi) - (\Delta W_N - \Delta w), \\ r_2 = (W_N - w) - (-\Delta\Phi_N + \Delta\phi) + \gamma(-\Phi_N + \phi) + (g(\phi)q - g(\Phi_N)Q_N), \\ r_3 = (\partial_t Q_N - \partial_t q) - \frac{1}{2}(g(\Phi_N)\partial_t\Phi_N - g(\phi)\partial_t\phi). \end{cases} \tag{36}$$

We observe that

$$\|\partial_t(\Phi_N - \phi)\|_2 = \|\mathcal{I}_N(\partial_t(\Phi_N - \phi))\|_{L^2} \le \|\partial_t(\Phi_N - \phi)\|_{L^2} + \|\partial_t(\mathcal{I}_N\phi - \phi)\|_{L^2}, \tag{37}$$

$$\|\partial_t(Q_N - q)\|_2 = \|\mathcal{I}_N(\partial_t(Q_N - q))\|_{L^2} \le \|\partial_t(Q_N - q)\|_{L^2} + \|\partial_t(\mathcal{I}_N q - q)\|_{L^2}. \tag{38}$$

Thus, we arrive at

$$\|\partial_t(\Phi_N - \phi)\|_2 \le Ch^m\|\partial_t\phi\|_{H^m}, \|\partial_t(Q_N - q)\|_2 \le Ch^m\|\partial_t q\|_{H^m}. \tag{39}$$

Using the similar arguments, we have

$$\|\Delta(W_N - w)\|_2 \le Ch^m\|w\|_{H^{m+2}}, \quad \|W_N - w\|_2 \le Ch^m\|w\|_{H^m}, \tag{40}$$

$$\|\Delta(\Phi_N - \phi)\|_2 \le Ch^m\|\phi\|_{H^{m+2}}, \quad \|\Phi_N - \phi\|_2 \le Ch^m\|\phi\|_{H^m}. \tag{41}$$

For the nonlinear term we find

$$\|g(\phi)q - g(\Phi_N)Q_N\|_{L^2} \le \|q\|_{L^\infty}\|g(\phi) - g(\Phi_N)\|_{L^2} + \|g(\Phi_N)\|_{L^\infty}\|q - Q_N\|_{L^2}. \tag{42}$$

Note that

$$\|Q_N - q\|_{L^2} \le Ch^m\|q\|_{H^m}, \tag{43}$$

$$\|g(\Phi_N) - g(\phi)\|_{L^2} \le C\|g'(\theta)\|_{L^\infty}\|\Phi_N - \phi\|_{L^2} \le C\|\Phi_N - \phi\|_{L^2}, \tag{44}$$

$$\|g(\phi)\partial_t q - g(\Phi_N)\partial_t Q_N\|_{L^2} \le \|\partial_t q\|_{L^\infty}\|g(\phi) - g(\Phi_N)\|_{L^2} + \|g(\Phi_N)\|_{L^\infty}\|\partial_t q - \partial_t Q_N\|_{L^2}. \tag{45}$$

Then, we can derive the following results

$$\begin{aligned}\|g(\phi)q - g(\Phi_N)Q_N\|_2 =& \|\mathcal{I}_N(g(\phi)q - g(\Phi_N)Q_N)\|_{L^2}\\ \le& \|g(\phi)q - g(\Phi_N)Q_N\|_{L^2} + \|g(\phi)q - \mathcal{I}_N(g(\phi)q)\|_{L^2}\\ &+ \|g(\Phi_N)Q_N - \mathcal{I}_N(g(\Phi_N)Q_N)\|_{L^2}\\ \le& Ch^m(\|\phi\|_{H^m} + \|f(\phi)\|_{H^m}),\end{aligned} \tag{46}$$

$$\begin{aligned}\|g(\phi)\partial_t\phi - g(\Phi_N)\partial_t\Phi_N\|_2 =& \|\mathcal{I}_N(g(\phi)\partial_t\phi - g(\Phi_N)\partial_t\Phi_N)\|_{L^2}\\ \le& \|g(\phi)\partial_t\phi - g(\Phi_N)\partial_t\Phi_N\|_{L^2} + \|g(\phi)\partial_t\phi - \mathcal{I}_N(g(\phi)\partial_t\phi)\|_{L^2}\\ &+ \|g(\Phi_N)\partial_t\Phi_N - \mathcal{I}_N(g(\Phi_N)\partial_t\Phi_N)\|_{L^2}\\ \le& Ch^m(\|\phi\|_{H^m} + \|\partial_t\phi\|_{H^m} + \|g(\phi)\partial_t\phi\|_{H^m}).\end{aligned} \tag{47}$$

Combining the equations above, we derive at

$$\|r_i\|_2 \le Ch^m, \quad i = 1, 2, 3. \tag{48}$$

Theorem 3.1. *Suppose (Φ_N, W_N, Q_N) as the approximation solution constructed by (33), denote (Φ, W, Q) be its discrete interpolation, then we arrive at*

$$\begin{cases}\frac{\Phi^{n+1}-\Phi^n}{\delta t} = D_N^2\Big(\frac{W^{n+1}+W^n}{2}\Big) + R_1^{n+\frac{1}{2}},\\ \frac{W^{n+1}+W^n}{2} = -D_N^2\Big(\frac{\Phi^{n+1}+\Phi^n}{2}\Big) + \gamma\frac{\Phi^{n+1}+\Phi^n}{2} + g(\Phi^{n+\frac{1}{2}})\frac{Q^{n+1}+Q^n}{2} + R_2^{n+\frac{1}{2}},\\ \frac{Q^{n+1}-Q^n}{\delta t} = \frac{1}{2}g(\Phi^{n+\frac{1}{2}})\frac{\Phi^{n+1}-\Phi^n}{\delta t} + R_3^{n+\frac{1}{2}},\end{cases} \tag{49}$$

where $\Phi^n = \Phi(t_n)$, $W^n = W(t_n)$, $Q^n = Q(t_n)$, and $R_i^{n+\frac{1}{2}} (i = 1, 2, 3)$ satisfies

$$\|R_i\|_{l^2(0,T;l^2)} := \Big(\delta t\sum_{k=0}^{K}\|R_i^{k+1}\|_2^2\Big)^{\frac{1}{2}} \le C((\delta t)^2 + h^m). \tag{50}$$

Proof. Let us introduce the notations as follows

$$\begin{aligned}
E_1^{n+\frac{1}{2}} =& \frac{\Phi^{n+1}-\Phi^n}{\delta t}, & E_{1e}^{n+\frac{1}{2}} =& \partial_t\Phi_N(t_{n+\frac{1}{2}}),\\
E_2^{n+\frac{1}{2}} =& D_N^2\Big(\frac{W^{n+1}+W^n}{2}\Big), & E_{2e}^{n+\frac{1}{2}} =& \Delta W_N(t_{n+\frac{1}{2}}),\\
E_3^{n+\frac{1}{2}} =& \frac{W^{n+1}+W^n}{2}, & E_{3e}^{n+\frac{1}{2}} =& W_N(t_{n+\frac{1}{2}}),\\
E_4^{n+\frac{1}{2}} =& D_N^2\Big(\frac{\Phi^{n+1}+\Phi^n}{2}\Big), & E_{4e}^{n+\frac{1}{2}} =& \Delta\Phi_N(t_{n+\frac{1}{2}}),\\
E_5^{n+\frac{1}{2}} =& \frac{\Phi^{n+1}+\Phi^n}{2}, & E_{5e}^{n+\frac{1}{2}} =& \Phi_N(t_{n+\frac{1}{2}}),\\
E_6^{n+\frac{1}{2}} =& g(\Phi^{n+\frac{1}{2}})\frac{Q^{n+1}+Q^n}{2}, & E_{6e}^{n+\frac{1}{2}} =& g(\Phi_N(t_{n+\frac{1}{2}}))Q_N(t_{n+\frac{1}{2}}),\\
E_7^{n+\frac{1}{2}} =& \frac{Q^{n+1}-Q^n}{\delta t}, & E_{7e}^{n+\frac{1}{2}} =& \partial_t Q_N(t_{n+\frac{1}{2}}),\\
E_8^{n+\frac{1}{2}} =& g(\Phi^{n+\frac{1}{2}})\frac{\Phi^{n+1}-\Phi^n}{\delta t}, & E_{8e}^{n+\frac{1}{2}} =& g(\Phi_N(t_{n+\frac{1}{2}}))\partial_t\Phi_N(t_{n+\frac{1}{2}}).
\end{aligned} \tag{51}$$

In turn, application of discrete summation in Ω leads to

$$\|E_1 - \mathcal{I}_N E_{1e}\|_{l^2(0,T;l^2)} \le C(\delta t)^2\|\Phi_N\|_{H^3(0,T;L^2)} \le C(\delta t)^2\|\phi\|_{H^3(0,T;L^2)}, \tag{52}$$

$$\|E_2 - \mathcal{I}_N E_{2e}\|_{l^2(0,T;l^2)} \le C(\delta t)^2\|W_N\|_{H^2(0,T;H^2)} \le C(\delta t)^2\|w\|_{H^2(0,T;H^2)}, \tag{53}$$

$$\|E_3 - \mathcal{I}_N E_{3e}\|_{l^2(0,T;l^2)} \le C(\delta t)^2\|W_N\|_{H^2(0,T;L^2)} \le C(\delta t)^2\|w\|_{H^2(0,T;L^2)}, \tag{54}$$

$$\|E_4 - \mathcal{I}_N E_{4e}\|_{l^2(0,T;l^2)} \le C(\delta t)^2\|\Phi_N\|_{H^2(0,T;H^2)} \le C(\delta t)^2\|\phi\|_{H^2(0,T;H^2)}, \tag{55}$$

$$\|E_5 - \mathcal{I}_N E_{5e}\|_{l^2(0,T;l^2)} \le C(\delta t)^2\|\Phi_N\|_{H^2(0,T;L^2)} \le C(\delta t)^2\|\phi\|_{H^2(0,T;L^2)}. \tag{56}$$

For the nonlinear $E_6^{n+\frac{1}{2}}, E_{6e}^{n+\frac{1}{2}}$, we have the following estimate

$$\begin{aligned}\left\|E_6^{n+\frac{1}{2}}-\mathcal{I}_N\left(g(\Phi_N^{n+\frac{1}{2}})\frac{Q_N^{n+1}+Q_N^n}{2}\right)\right\|_2 \leq & Ch^m\left\|g(\Phi_N^{n+\frac{1}{2}})\frac{Q_N^{n+1}+Q_N^n}{2}\right\|_{H^m}\\ \leq & Ch^m\left(\|f(\Phi_N)\|_{L^\infty(0,T;H^m)}+\|\Phi_N\|_{L^\infty(0,T;H^m)}\right).\end{aligned} \tag{57}$$

Note that

$$\begin{aligned}&\left\|\mathcal{I}_N\left(g(\Phi_N^{n+\frac{1}{2}})\frac{Q_N^{n+1}+Q_N^n}{2}-E_{6e}^n\right)\right\|_2\\ \leq & C(\delta t)^2\left(\|f(\Phi_N)\|_{L^\infty(0,T;L^\infty)}+\|\Phi_N\|_{L^\infty(0,T;L^\infty)}\right)\|Q_N\|_{H^2(0,T;L^2)}.\end{aligned} \tag{58}$$

Then, we obtain the following

$$\|E_6-\mathcal{I}_N(E_{6e})\|_{l^2(0,T;l^2)}\leq C((\delta t)^2+h^m). \tag{59}$$

Similarly, we can obtain that

$$\|E_7-\mathcal{I}_N E_{7e}\|_{l^2(0,T;l^2)}\leq C(\delta t)^2\|Q_N\|_{H^3(0,T;L^2)}\leq C(\delta t)^2\|q\|_{H^3(0,T;L^2)}. \tag{60}$$

For the last two nonlinear terms, we arrive at

$$\begin{aligned}&\left\|E_8^{n+\frac{1}{2}}-\mathcal{I}_N\left(g(\Phi_N^{n+\frac{1}{2}})\frac{\Phi_N^{n+1}-\Phi_N^n}{\delta t}\right)\right\|_2\\ \leq & Ch^m\left\|g(\Phi_N^{n+\frac{1}{2}})\frac{\Phi_N^{n+1}-\Phi_N^n}{\delta t}\right\|_{H^m}\\ \leq & Ch^m\left(\|f(\Phi_N)\|_{L^\infty(0,T;H^{m+2})}+\|\Phi_N\|_{L^\infty(0,T;H^{m+2})}\right)\|\Phi_N\|_{H^1(0,T;H^m)},\end{aligned} \tag{61}$$

and

$$\begin{aligned}&\left\|\mathcal{I}_N\left(g(\Phi_N^{n+\frac{1}{2}})\frac{\Phi_N^{n+1}-\Phi_N^n}{\delta t}-E_{8e}^n\right)\right\|_2\\ \leq & C(\delta t)^2\left(\|f(\Phi_N)\|_{L^\infty(0,T;L^\infty)}+\|\Phi_N\|_{L^\infty(0,T;L^\infty)}\right)\|\Phi_N\|_{H^3(0,T;L^2)}.\end{aligned} \tag{62}$$

That is

$$\|E_8-\mathcal{I}_N(E_{8e})\|_{l^2(0,T;l^2)}\leq C((\delta t)^2+h^m). \tag{63}$$

Combining the estimates above, the consistency analysis (50) is completed. □

Lemma 3.2. *Given (a) $\exists B$ such that $F(x)-\frac{\gamma}{2}x^2+B>0$, $\forall x\in(-\infty,+\infty)$; (b) $F(x)\in C^2(-\infty,\infty)$; (c) there exists a positive constant C_0 such that*

$$\max_{n\leq k}\left\{\|\Phi^n\|_{L^\infty},\|\phi^n\|_{L^\infty}\right\}\leq C_0. \tag{64}$$

It holds

$$\max_{n\leq k}\left\{\|F_1(\chi^n)\|_{L^\infty},\|f_1(\chi^n)\|_{L^\infty},\|f_1'(\chi^n)\|_{L^\infty},\|\sqrt{F_1(\chi^n+B)}\|_{L^\infty}\right\}\leq C_1, \tag{65}$$

with $F_1(x)=F(x)-\frac{\gamma}{2}x^2, f_1=F_1', \chi^n=\varepsilon\Phi^n+(1-\varepsilon)\phi^n, \varepsilon\in[0,1]$. Moreover, we have

$$\|g(\Phi^n)-g(\phi^n)\|_2\leq C_2\|\Phi^n-\phi^n\|_2. \tag{66}$$

here C_2 is a constant which dependent on C_0, C_1, B.

Proof. Follow assumption (c), we know that χ^n is uniformly bounded, combine with assumption (b), we can obtain (65). By using the similar arguments in (44), we arrive at (66). □

Lemma 3.3. *Given (a) $\exists B$ such that $F(x)-\frac{\gamma}{2}x^2+B>0$, $\forall x\in(-\infty,+\infty)$; (b) $F(x)\in C^3(-\infty,+\infty)$; (c) there exists a positive constant C_3 such that*

$$\max_{n\leq k}\left\{\|\Phi^n\|_{L^\infty},\|\phi^n\|_{L^\infty}\right\}\leq C_3.$$

The following inequalities hold

$$\begin{aligned}&\max_{n\le k}\left\{\|F_1(\chi^n)\|_{L^\infty}, \|f_1(\chi^n)\|_{L^\infty}, \|f_1'(\chi^n)\|_{L^\infty}, \|f_1''(\chi^n)\|_{L^\infty}, \|\sqrt{F(\chi^n+B)}\|_{L^\infty}\right\}\le C_4,\\ &\|D_N g(\Phi^n)-D_N g(\phi^n)\|_2\le C_5(\|D_N(\Phi^n-\phi^n)\|_2+\|\Phi^n-\phi^n\|_2),\end{aligned}\tag{67}$$

where C_5 is only dependent on C_4, C_3, B.

Lemma 3.4. *Denote $\{u^n\}_{n=0}^{k+1}$ be sequences of function on Ω, then we have*

$$\|u^{k+1}\|\le\sum_{n=0}^{k}\|u^{n+1}+u^n\|+\|u^0\|.$$

Some regularity assumption

$$\begin{cases}\phi\in L^\infty(0,T;H^2(\Omega))\cap L^\infty(0,T;W^{1,\infty}(\Omega)), \quad \partial_t\phi,\partial_t q\in L^2(0,T;H^1(\Omega))\cap L^\infty(0,T;L^\infty(\Omega)),\\ q\in L^\infty(0,T;W^{1,\infty}(\Omega)), \quad \partial_t^2 q,\partial_t^3 q,\partial_t^2 q,\partial_t^3\phi\in L^2(0,T;L^2(\Omega)), \quad w\in L^2(0,T;H^2(\Omega)).\end{cases}\tag{68}$$

In order to prove the error estimate, we define ν, such that

$$\nu=\max_{0\le t\le T}\|\Phi(t)\|_{L^\infty}+1.$$

Lemma 3.5. *Suppose $\exists B$ such that $F(x)-\frac{\gamma}{2}x^2+B>0$ for all $x\in(-\infty,+\infty)$, $F(x)\in C^3(-\infty,+\infty)$ and the exact solution satisfied some regularity assumptions (68), and there is a given constant τ_0 and h_0, when $\delta t<\tau_0, h<h_0$, for any $k=0,1,\dots,[T/dt]$, we have the following results*

$$\|\phi^k\|_{L^\infty}\le\nu.\tag{69}$$

Proof. We present the proof using mathematical induction. When $n=0$, it is easy to verify that $\|\phi^0\|_{L^\infty}\le\nu$. Suppose $\|\phi^n\|_{L^\infty}\le\nu$ for $n\le k$ holds. Next we will show $\|\phi^{k+1}\|_{L^\infty}\le\nu$ still valid. First we define the error function

$$\widetilde{e}_\phi^n=\Phi^n-\phi^n,\quad \widetilde{e}_w^n=W^n-w^n,\quad \widetilde{e}_q^n=Q^n-q^n.\tag{70}$$

Subtracting (17) from (49) yields

$$\begin{cases}\frac{\widetilde{e}_\phi^{n+1}-\widetilde{e}_\phi^n}{\delta t}=D_N^2\left(\frac{\widetilde{e}_w^{n+1}+\widetilde{e}_w^n}{2}\right)+R_1^{n+\frac12},\\ \frac{\widetilde{e}_w^{n+1}+\widetilde{e}_w^n}{2}=-D_N^2\left(\frac{\widetilde{e}_\phi^{n+1}+\widetilde{e}_\phi^n}{2}\right)+\gamma\frac{\widetilde{e}_\phi^{n+1}+\widetilde{e}_\phi^n}{2}+\mathcal{X}+R_2^{n+\frac12},\\ \frac{\widetilde{e}_q^{n+1}-\widetilde{e}_q^n}{\delta t}=\frac12\mathcal{Y}+R_3^{n+\frac12},\end{cases}\tag{71}$$

where

$$\mathcal{X}:=\left(g(\Phi^{n+\frac12})\frac{Q^{n+1}+Q^n}{2}-g(\phi^*)\frac{q^{n+1}+q^n}{2}\right),\tag{72}$$

$$\mathcal{Y}:=\left(g(\Phi^{n+\frac12})\frac{\Phi^{n+1}-\Phi^n}{\delta t}-g(\phi^*)\frac{\phi^{n+1}-\phi^n}{\delta t}\right).\tag{73}$$

We note a $W^{2,\infty}$ bound for the constructed solution

$$\|\Phi_N\|_{L^\infty(0,T;W^{2,\infty})}\le C,\quad \text{i.e. } \|\Phi^n\|_{L^\infty}\le C,\quad \|\nabla\Phi^n\|_{L^\infty}\le C.\tag{74}$$

Taking a discrete inner product with the first equation in (71) with error function $2\delta t(\widetilde{e}_w^{n+1}+\widetilde{e}_w^n)$ gives

$$\left\langle\widetilde{e}_\phi^{n+1}-\widetilde{e}_\phi^n,\widetilde{e}_w^{n+1}+\widetilde{e}_w^n\right\rangle=-\delta t\|D_N(\widetilde{e}_w^{n+1}+\widetilde{e}_w^n)\|_2^2+2\delta t\left\langle R_1^{n+\frac12},\widetilde{e}_w^{n+1}+\widetilde{e}_w^n\right\rangle.\tag{75}$$

Taking a discrete inner product with the second equation of (71) by the error function $2(\widetilde{e}_\phi^{n+1}-\widetilde{e}_\phi^n), 2\delta t(\widetilde{e}_w^{n+1}+\widetilde{e}_w^n)$ gives

$$\begin{aligned}\left\langle\widetilde{e}_w^{n+1}+\widetilde{e}_w^n,\widetilde{e}_\phi^{n+1}-\widetilde{e}_\phi^n\right\rangle=&\|D_N\widetilde{e}_\phi^{n+1}\|_2^2-\|D_N\widetilde{e}_\phi^n\|_2^2+\gamma(\|\widetilde{e}_\phi^{n+1}\|_2^2-\|\widetilde{e}_\phi^n\|_2^2)\\ &+2\left\langle\mathcal{X},\widetilde{e}^{n+1}-\widetilde{e}^n\right\rangle+2\left\langle R_2^{n+\frac12},\widetilde{e}^{n+1}-\widetilde{e}^n\right\rangle,\end{aligned}\tag{76}$$

$$\begin{aligned}\delta t\|\widetilde{e}_w^{n+1}+\widetilde{e}_w^n\|_2^2=&2\delta t\left\langle-D_N^2\left(\frac{\widetilde{e}_\phi^{n+1}+\widetilde{e}_\phi^n}{2}\right),\widetilde{e}_w^{n+1}+\widetilde{e}_w^n\right\rangle+\gamma\delta t\left\langle\widetilde{e}_\phi^{n+1}+\widetilde{e}_\phi^n,\widetilde{e}_w^{n+1}+\widetilde{e}_w^n\right\rangle\\ &+2\delta t\left\langle\mathcal{X},\widetilde{e}_w^{n+1}+\widetilde{e}_w^n\right\rangle+2\delta t\left\langle R_2^{n+\frac12},\widetilde{e}_w^{n+1}+\widetilde{e}_w^n\right\rangle.\end{aligned}\tag{77}$$

Taking a discrete inner product with the third equation of (71) by the error function $2\delta t(\widetilde{e}_q^{n+1}+\widetilde{e}_q^{n})$ gives

$$2\|\widetilde{e}_q^{n+1}\|_2^2-2\|\widetilde{e}_q^{n}\|_2^2=\delta t\Big\langle \mathcal{Y},\widetilde{e}_q^{n+1}+\widetilde{e}_q^{n}\Big\rangle+2\delta t\Big\langle R_3^{n+\frac{1}{2}},\widetilde{e}_q^{n+1}+\widetilde{e}_q^{n}\Big\rangle. \tag{78}$$

Note that

$$\mathcal{X}=\frac{Q^{n+1}+Q^{n}}{2}(g(\Phi^{n+\frac{1}{2}})-g(\phi^*))+g(\phi^*)\frac{e_q^{n+1}+e_q^{n}}{2},$$

and

$$\mathcal{Y}=\frac{\Phi^{n+1}-\Phi^{n}}{\delta t}(g(\Phi^{n+\frac{1}{2}})-g(\phi^*))+g(\phi^*)\frac{e_\phi^{n+1}-e_\phi^{n}}{\delta t}.$$

The inner product associated by the truncation error can be handled in a straightforward way:

$$2\Big\langle R_1^{n+\frac{1}{2}},\widetilde{e}_w^{n+1}+\widetilde{e}_w^{n}\Big\rangle\le C\|R_1^{n+\frac{1}{2}}\|_2^2+\frac{1}{6}\|\widetilde{e}_w^{n+1}+\widetilde{e}_w^{n}\|_2^2, \tag{79}$$

$$\begin{aligned}-2\Big\langle R_2^{n+\frac{1}{2}},\widetilde{e}^{n+1}-\widetilde{e}^{n}\Big\rangle&=-\delta t\Big\langle R_2^{n+\frac{1}{2}},D_N^2\frac{\widetilde{e}_w^{n+1}+\widetilde{e}_w^{n}}{2}+R_1^{n+\frac{1}{2}}\Big\rangle\\&\le C\delta t\Big(\|R_1^{n+\frac{1}{2}}\|_2^2+\|R_2^{n+\frac{1}{2}}\|_2^2+\|D_NR_2^{n+\frac{1}{2}}\|_2^2\Big)+\frac{\delta t}{4}\|D_N(\widetilde{e}_w^{n+1}+\widetilde{e}_w^{n})\|_2^2,\end{aligned} \tag{80}$$

$$2\Big\langle R_3^{n+\frac{1}{2}},\widetilde{e}_q^{n+1}+\widetilde{e}_q^{n}\Big\rangle\le\|R_3^{n+\frac{1}{2}}\|_2^2+\|\widetilde{e}_q^{n+1}+\widetilde{e}_q^{n}\|_2^2. \tag{81}$$

Using similar techniques, we find

$$\Big\langle -D_N^2(\widetilde{e}_\phi^{n+1}+\widetilde{e}_\phi^{n}),\widetilde{e}_w^{n+1}+\widetilde{e}_w^{n}\Big\rangle\le C\|D_N(\widetilde{e}_\phi^{n+1}+\widetilde{e}_\phi^{n})\|_2^2+\frac{1}{4}\|D_N(\widetilde{e}_w^{n+1}+\widetilde{e}_w^{n})\|_2^2, \tag{82}$$

$$\Big\langle \widetilde{e}_\phi^{n+1}+\widetilde{e}_\phi^{n},\widetilde{e}_w^{n+1}+\widetilde{e}_w^{n}\Big\rangle\le C\|\widetilde{e}_\phi^{n+1}+\widetilde{e}_\phi^{n}\|_2^2+\frac{1}{6}\|\widetilde{e}_w^{n+1}+\widetilde{e}_w^{n}\|_2^2, \tag{83}$$

$$\begin{aligned}2\Big\langle \mathcal{X}+R_2^{n+\frac{1}{2}},\widetilde{e}_w^{n+1}+\widetilde{e}_w^{n}\Big\rangle&\le C\Big(\|\widetilde{e}_q^{n+1}+\widetilde{e}_q^{n}\|_2^2+\|R_2^{n+\frac{1}{2}}\|_2^2+\|\widetilde{e}_\phi^{n}\|_2^2+\|\widetilde{e}_\phi^{n-1}\|_2^2+\delta t^4\Big)\\&\quad+\frac{1}{6}\|\widetilde{e}_w^{n+1}+\widetilde{e}_w^{n}\|_2^2.\end{aligned} \tag{84}$$

For the nonlinear term, we find

$$\begin{aligned}&-2\Big\langle \mathcal{X},\widetilde{e}_\phi^{n+1}-\widetilde{e}_\phi^{n}\Big\rangle+\delta t\Big\langle \mathcal{Y},\widetilde{e}_q^{n+1}+\widetilde{e}_q^{n}\Big\rangle\\&=-2\Big\langle\frac{Q^{n+1}+Q^{n}}{2}(g(\Phi^{n+\frac{1}{2}})-g(\phi^*))+g(\phi^*)\frac{e_q^{n+1}+e_q^{n}}{2},\widetilde{e}_\phi^{n+1}-\widetilde{e}_\phi^{n}\Big\rangle\\&\quad+\delta t\Big\langle\frac{\Phi^{n+1}-\Phi^{n}}{\delta t}(g(\Phi^{n+\frac{1}{2}})-g(\phi^*))+g(\phi^*)\frac{e_\phi^{n+1}-e_\phi^{n}}{\delta t},\widetilde{e}_q^{n+1}+\widetilde{e}_q^{n}\Big\rangle\\&=-2\delta t\Big\langle\frac{Q^{n+1}+Q^{n}}{2}(g(\Phi^{n+\frac{1}{2}})-g(\phi^*)),D_N^2\Big(\frac{\widetilde{e}_w^{n+1}+\widetilde{e}_w^{n}}{2}\Big)+R_1^{n+\frac{1}{2}}\Big\rangle\\&\quad+\delta t\Big\langle\frac{\Phi^{n+1}-\Phi^{n}}{\delta t}(g(\Phi^{n+\frac{1}{2}})-g(\phi^*)),\widetilde{e}_q^{n+1}+\widetilde{e}_q^{n}\Big\rangle\\&\le C\delta t\Big(\|R_1^{n+\frac{1}{2}}\|_2^2+\|\widetilde{e}_\phi^{n}\|_2^2+\|\widetilde{e}_\phi^{n-1}\|_2^2+(\delta t)^4+\|D_N\widetilde{e}_\phi^{n}\|_2^2+\|D_N\widetilde{e}_\phi^{n-1}\|_2^2+\|\widetilde{e}_q^{n+1}+\widetilde{e}_q^{n}\|_2^2\Big)\\&\quad+\frac{\delta t}{4}\|D_N(\widetilde{e}_w^{n+1}+\widetilde{e}_w^{n})\|_2^2.\end{aligned} \tag{85}$$

Combining with (75)–(85), we arrive at

$$\begin{aligned}&\|D_N\widetilde{e}_\phi^{n+1}\|_2^2-\|D_N\widetilde{e}_\phi^{n}\|_2^2+\gamma(\|\widetilde{e}_\phi^{n+1}\|_2^2-\|\widetilde{e}_\phi^{n}\|_2^2)\\&\quad+2(\|\widetilde{e}_q^{n+1}\|_2^2-\|\widetilde{e}_q^{n}\|_2^2)+\frac{\delta t}{2}\Big(\|D_N(\widetilde{e}_w^{n+1}+\widetilde{e}_w^{n})\|_2^2+\|\widetilde{e}_w^{n+1}+\widetilde{e}_w^{n}\|_2^2\Big)\\&\le C\delta t((\delta t)^4+h^{2m})+C\delta t\Big(\|\widetilde{e}_\phi^{n}\|_2^2+\|\widetilde{e}_\phi^{n-1}\|_2^2+\|D_N\widetilde{e}_\phi^{n}\|_2^2+\|D_N\widetilde{e}_\phi^{n-1}\|_2^2\\&\quad+\|\widetilde{e}_q^{n+1}+\widetilde{e}_q^{n}\|_2^2+(\delta t)^4+\|D_N(\widetilde{e}_\phi^{n+1}+\widetilde{e}_\phi^{n})\|_2^2+\|\widetilde{e}_\phi^{n+1}+\widetilde{e}_\phi^{n}\|_2^2\Big).\end{aligned}$$

Summing up for $n = 1, \ldots, k$, we have

$$\widetilde{E}^{k+1} + \frac{\delta t}{2}\sum_{n=1}^{k}\Big(\|D_N(\widetilde{e}_w^{n+1} + \widetilde{e}_w^{n})\|_2^2 + \|\widetilde{e}_w^{n+1} + \widetilde{e}_w^{n}\|_2^2\Big) \le \widetilde{E}^1 + C((\delta t)^2 + h^m)^2 + C\delta t\sum_{n=1}^{k}\widetilde{E}^{n+1}, \tag{86}$$

with

$$\widetilde{E}^n = \|D_N\widetilde{e}_\phi^n\|_2^2 + \gamma\|\widetilde{e}_\phi^n\|_2^2 + 2\|\widetilde{e}_q^n\|_2^2.$$

For the first step, it is easy to verify that

$$\widetilde{E}^1 \le C((\delta t)^2 + h^m)^2. \tag{87}$$

Applying discrete Gronwall inequality gives

$$\widetilde{E}^{k+1} + \frac{\delta t}{2}\sum_{n=1}^{k}\Big(\|D_N(\widetilde{e}_w^{n+1} + \widetilde{e}_w^{n})\|_2^2 + \|\widetilde{e}_w^{n+1} + \widetilde{e}_w^{n}\|_2^2\Big) \le C((\delta t)^2 + h^m)^2. \tag{88}$$

From second equation in (71), we find

$$\|D_N^2(\widetilde{e}_\phi^{n+1} + \widetilde{e}_\phi^{n})\|_2^2 \le C\Big(\|\widetilde{e}_\phi^{n+1} + \widetilde{e}_\phi^{n}\|_2^2 + \|\widetilde{e}_w^{n+1} + \widetilde{e}_w^{n}\|_2^2 + \|\mathcal{X}\|_2^2 + \|R_2^{n+\frac{1}{2}}\|_2^2\Big). \tag{89}$$

From Lemma 3.4, along with (88) and (89), we find that

$$\|D_N^2\widetilde{e}_\phi^{k+1}\|_2 \le \sum_{n=0}^{k}\|D_N^2(\widetilde{e}_\phi^{n+1} + \widetilde{e}_\phi^{n})\|_2 \le C(\delta t + \delta t^{-1}h^m). \tag{90}$$

Moreover, we have the following

$$\begin{aligned}\|\phi^{k+1}\|_{L^\infty} \le& \|\widetilde{e}_\phi^{k+1}\|_{L^\infty} + \|\Phi^{k+1}\|_{L^\infty}\\ \le& C\|e_\phi^{k+1}\|_{H^1}^{\frac{1}{2}}\|e_\phi^{k+1}\|_{H^2}^{\frac{1}{2}} + \|\Phi^{k+1}\|_{L^\infty}\\ \le& \widetilde{C}((\delta t)^3 + \delta t h^m + \delta t^{-1}h^{2m})^{\frac{1}{2}} + \|\Phi^{k+1}\|_{L^\infty}.\end{aligned} \tag{91}$$

If $\widetilde{C}((\delta t)^3 + \delta t h^m + \delta t^{-1}h^{2m})^{\frac{1}{2}} \le 1$, we have

$$\|\phi^{k+1}\|_{L^\infty} \le 1 + \|\Phi^{k+1}\|_{L^\infty} \le \nu. \quad \square \tag{92}$$

Theorem 3.6. *Under the assumption of Lemma 3.5, we have*

$$\begin{aligned}&\|\phi(t_{k+1}) - \phi^{k+1}\|_{H^1} + \|q(\phi(t_{k+1})) - q(\phi^{k+1})\|_2\\ &+\delta t\sum_{n=0}^{k}\Big\|(w(t_{n+1}) + w(t_n)) - (w^{n+1} + w^n)\Big\|_{H^1} \le C((\delta t)^2 + h^m).\end{aligned} \tag{93}$$

Proof. Because $\|\phi^n\|_{L^\infty} \le \nu, \forall 0 \le n \le [T/\delta t]$, by the same way in Lemma 3.5, we obtained that

$$\widetilde{E}^{k+1} + \frac{\delta t}{2}\sum_{n=0}^{k}\Big(\|D_N(\widetilde{e}_w^{n+1} + \widetilde{e}_w^{n})\|_2^2 + \|\widetilde{e}_w^{n+1} + \widetilde{e}_w^{n}\|_2^2\Big) \le C((\delta t)^2 + h^m)^2. \tag{94}$$

Using the fact that

$$\begin{aligned}\|\phi(t_k) - \phi^k\|_{L^2} \le& \|\phi(t_k) - \Phi^k\|_{L^2} + \|\Phi^k - \phi^k\|_{L^2},\\ \|\nabla\phi(t_k) - D_N\phi^k\|_{L^2} \le& \|\nabla\phi(t_k) - \nabla\Phi^k\|_{L^2} + \|\nabla\Phi^k - D_N\Phi^k\|_{L^2} + \|D_N\Phi^k - D_N\phi^k\|_{L^2},\\ \|\nabla\Phi^k - D_N\Phi^k\|_{L^2} \le& \|\nabla\Phi^k - \mathcal{I}_N(\nabla\Phi^k)\|_{L^2} + \|\mathcal{I}_N(\nabla\Phi^k) - D_N\Phi^k\|_{L^2}.\end{aligned}$$

This is completes the proof.

4. Numerical examples

In this section, we present some numerical examples to verify our theoretical results. Notice the proof in the previous section does not rely on the specific bulk potential, so long as it is regular enough.

In the numerical example, we consider the double-well bulk potential $F(\phi) = \frac{1}{4}(\phi^2 - 1)^2$. Thus, the effective free energy is given as

$$E = \int_\Omega\Big(\frac{\varepsilon^2}{2}|\nabla\phi|^2 + \frac{1}{4}(\phi^2 - 1)^2\Big)d\mathbf{x}, \tag{95}$$

Table 1
The L^2 and L^∞ numerical errors for ϕ at time $t = 0.1$. They are computed by the scheme (17) using various temporal resolutions.

δt	L^2- Error for ϕ	Order	$L^\infty-$ Error for ϕ	Order
0.1	5.382847673102089		0.064224660088156	
0.05	3.011560406627883	0.84	0.043544456316727	0.56
0.025	1.485377707482468	1.02	0.024932830783236	0.80
0.0125	0.601548874665940	1.30	0.010949875468669	1.19
0.00625	0.191121667198677	1.65	0.003540887587754	1.63
0.003125	0.052354457904304	1.86	0.000968884572137	1.87
0.0015625	0.013549031245968	1.95	0.000250402613180	1.95
0.00078125	0.003435558619516	1.98	0.000063452340170	1.98
0.000390625	0.000864284575129	1.99	0.000015958073598	1.99
0.0001953125	0.000216700141005	1.99	0.000004000594657	2.00

Table 2
The L^2 and L^∞ numerical errors for q at time $t = 0.1$. They are computed by the scheme (17) using various temporal resolutions.

δt	L^2- Error for q	Order	$L^\infty-$ Error for q	Order
0.1	3.182110885713837		0.030974618534329	
0.05	1.431447443475112	1.15	0.018703864596920	0.73
0.025	0.586297237571693	1.29	0.009601528492512	0.96
0.0125	0.214385966336326	1.45	0.003937457227315	1.29
0.00625	0.065947460396376	1.70	0.001235000255575	1.67
0.003125	0.017949882223041	1.88	0.000335977369325	1.89
0.0015625	0.004637362290417	1.95	0.000086822780569	1.95
0.00078125	0.001175114043622	1.98	0.000021996188564	1.98
0.000390625	0.000295539519731	1.99	0.000005531083182	1.99
0.0001953125	0.000074089697926	2.00	0.000001386479378	2.00

and the corresponding Cahn–Hilliard equation reads as

$$\begin{cases} \partial_t \phi = \lambda \Delta \mu, \\ \mu = -\varepsilon^2 \Delta \phi + \phi^3 - \phi, \end{cases} \tag{96}$$

with periodic boundary condition, where λ is the mobility parameter, and ε is a parameter that controls the interfacial thickness.

4.1. Temporal and spacial convergence tests

First of all, we test the temporal and spacial convergence rates. We fix the domain as $\Omega = [0\ \ 1]^2$. And the parameters are chosen as $\lambda = 0.01$ and $\varepsilon = 0.01$. Introducing the auxiliary variable $q = \frac{1}{2}(\phi^2 - 1)$, we can reformulate the Cahn–Hilliard equation and utilize the proposed scheme thereafter.

For the temporal convergence test, we fix the meshes as $N_x = N_y = 256$ and initial profile $\phi(x, y, t = 0) = \sin(2\pi x)\sin(2\pi y)$. Since the analytical solution is not known, we pick the numerical solution with $\delta t = 10^{-6}$ as the benchmark solution. The error for ϕ in both $L^2(\Omega)$ and $L^\infty(\Omega)$ using different time steps is summarized in Table 1. We observe when the time step is small enough (saying $\delta t < 0.0015$), the numerical solution of ϕ reaches approximately second-order convergence in time, which shows strong agreement with our theoretical results.

Also, the numerical errors for the auxiliary variable q using different time steps are summarized in Table 2, which indicates that it reaches second-order accuracy in time as well.

Then we want to verify the spectral convergence rate in space. To avoid the temporal error affecting our study, we choose fixed, but refined, time step size $\delta t = 10^{-6}$, and we use the numerical solution with spatial resolution $N_x = N_y = 1024$ as the 'accurate' solution. The L^2 and L^∞ numerical errors for ϕ with different meshes 8^2, 16^2, 32^2, 64^2 and 128^2 are calculated. The numerical results are summarized in Table 3. We observe it reaches spectral convergence in space.

Besides, the numerical errors for the auxiliary variable q using various spatial resolutions are summarized in Table 4. We also observe that the numerical solution of q reaches spectral convergence in space as well.

Then, the CPU time with various temporal and spatial steps to calculate $\phi(x, y)$ at $t = 10$ are summarized in Table 5, indicating the effectiveness of the IEQ method in temporal discretization and Fourier pseudo-spectral in spatial discretization.

Table 3
The L^2 and L^∞ numerical errors for ϕ are computed using various spacial resolutions. Here we use fixed time step $\delta t = 10^{-6}$, and the error is calculated at time $t = 0.1$.

δx	L^2- Error for ϕ	Order	$L^\infty-$ Error for ϕ	Order
$\frac{1}{8}$	0.047992863063144		0.072344970776219	
$\frac{1}{16}$	0.007574170567587	2.85	0.009651137322507	2.69
$\frac{1}{32}$	0.000221462396449	4.82	0.000352470327596	4.80
$\frac{1}{64}$	0.000000962747435	8.04	0.000001425897338	8.05
$\frac{1}{128}$	0.000000000094892	13.60	0.000000000115794	13.80

Table 4
The L^2 and L^∞ numerical errors for q are computed using various spacial resolutions. Here we use fixed time step $\delta t = 10^{-6}$, and the error is calculated at time $t = 0.1$.

δx	L^2- Error for q	Order	$L^\infty-$ Error for q	Order
$\frac{1}{8}$	0.049062780958258		0.081703112179204	
$\frac{1}{16}$	0.007737225232038	2.84	0.010277382332508	2.99
$\frac{1}{32}$	0.000240957717925	4.80	0.000377147382304	4.80
$\frac{1}{64}$	0.000001038592048	8.03	0.000001546686298	8.05
$\frac{1}{128}$	0.000000000097732	13.62	0.000000000125793	13.50

Table 5
CPU time using various temporal and spatial steps to calculate ϕ to $t = 10$.

Meshes v.s. Time steps	0.01	0.005	0.0025	0.00125	0.000625
8	0.08085	0.126686	0.210256	0.339946	0.603604
16	0.243403	0.376907	0.538998	0.837921	1.284166
32	0.951075	1.246361	1.79219	2.736988	3.903051
64	3.905562	5.353976	8.2012	12.400856	19.462978
128	9.979772	13.442369	20.191874	31.157279	50.515492

4.2. Coarsening dynamics

Next, we conduct several other numerical tests on using the fully discrete scheme to study long-time predictions of coarsening dynamics.

In the first example, we study the coarsening dynamics following the same setting as [43], where we use the initial profile $\phi_0(x, y) = 0.05 \sin(x) \sin(y)$, set $\lambda = 1$, $\varepsilon = 0.1$, and pick the domain $\Omega = [0\ \ 2\pi]^2$. Also, a fine spacial mesh $N_x = N_y = 256$ and temporal step size $\delta t = 10^{-3}$ is used to capture the evolution dynamics accurately. The profile of ϕ at different time slots are summarized in Fig. 1, where it agrees qualitatively well with the simulation in [43] using the same parameters and initial conditions.

The energy evolution with time is plotted in Fig. 2, where we observe it decreases in time, i.e., it verifies that the scheme is energy stable (thus it agrees well with our theoretical result). Also, this energy prediction agrees well with the simulation results in [43].

Next, to verify the accuracy of our numerical schemes quantitatively, we use the proposed full discrete scheme to investigate the benchmark problem of coarsening dynamics following the same setting as [44]. In details, we choose the domain $\Omega = [0\ \ 4\pi]^2$ and parameters $\lambda = 0.02$, $\varepsilon = 0.05$. In the simulation, we pick spatial meshes $N_x = N_y = 256$ and the time step $\delta t = 10^{-3}$. The coarsening dynamics are summarized in Fig. 3.

It is known in [44] that the free energy of this benchmark problem decays following a power law $E(t) \approx O(t^{-\frac{1}{3}})$. the free energy evolution with time using the proposed full discrete scheme are summarized in Fig. 4. From the numerical results, we observe that the slope is approximate $-\frac{1}{3}$, i.e., it agrees well with the report in [44].

5. Conclusion

In this paper, we present rigorous error analysis of a full discrete linear scheme for solving the Cahn–Hilliard type equation, which is also shown to be energy stable and uniquely solvable. In specific, we use the IEQ technique to transform the CH type equation, the Crank–Nicolson finite difference method for temporal discretization and Fourier pseudo-spectral method for spatial discretization. The resulted full discrete scheme is proved to be second-order convergent in time

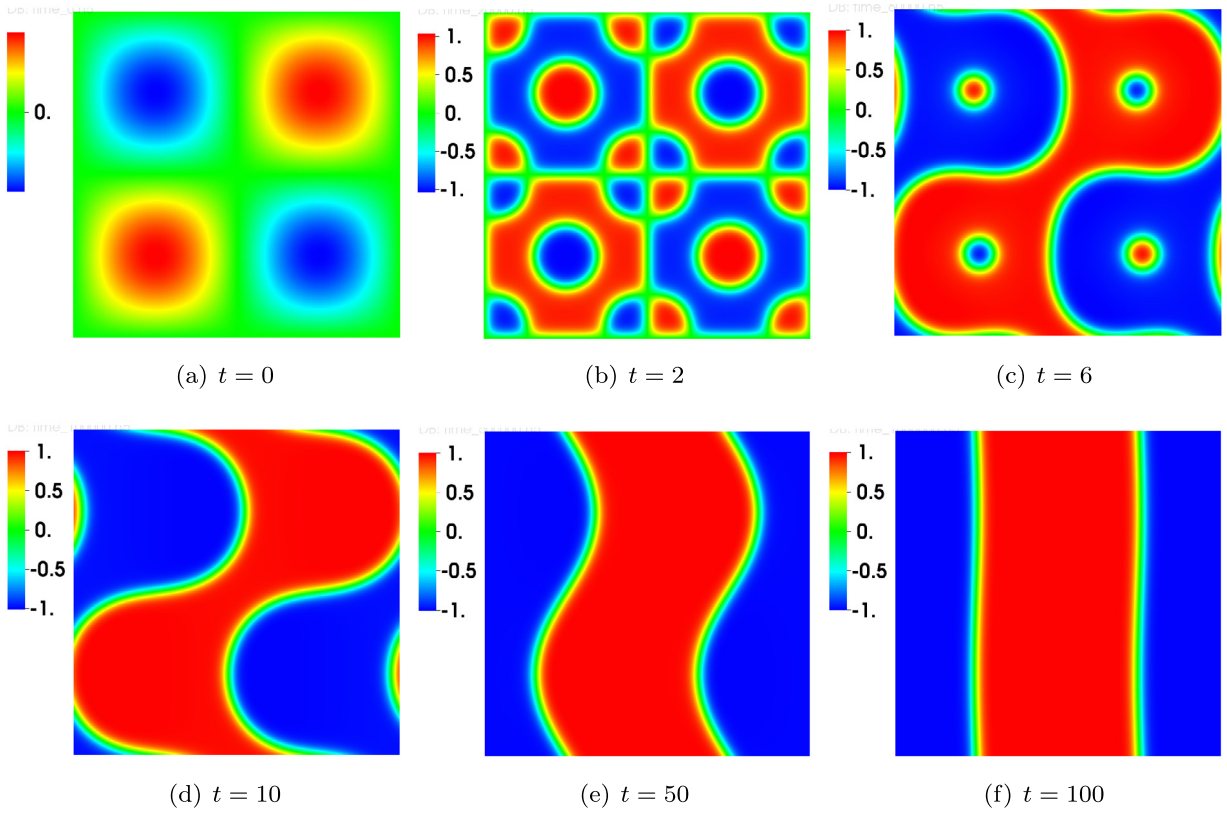

Fig. 1. The isolines of numerical solutions of the function ϕ for the Cahn–Hilliard equation using the full discrete scheme (17). The time step is $\delta t = 0.001$. Snapshots are taken at $t = 0, 2, 6, 10, 50, 100$, respectively. The predicted coarsening dynamics agrees well with the report in literature [43].

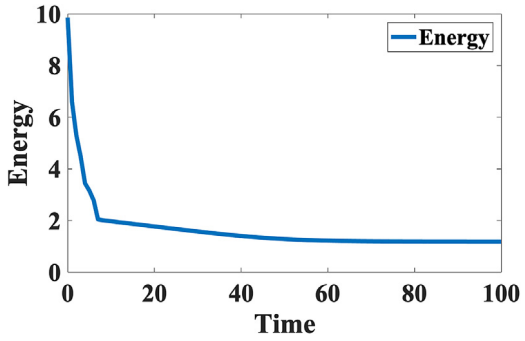

Fig. 2. Energy evolution of coarsening predicted by the Cahn–Hilliard equation.

and spectral convergent in space, making it an effective scheme for simulating long-time dynamics using the Cahn–Hilliard model. Numerical tests in several situations are presented, verifying our theoretical results, demonstrating the effectiveness of the proposed full discrete scheme as well.

Acknowledgments

Yuezheng Gong work is partially supported by the NSF of Jiangsu Province, China (Grant No. BK20180413) and NSFC, China 11801269. Jia Zhao work is partially supported by National Science Foundation (NSF), USA DMS-1816783. The work of Jun Zhang is supported by the NSFC, China (No. 11901132), the China Scholarship Council (No. 201908525061), and Guizhou Key Laboratory of Big Data Statistics Analysis, China (No. BDSA20190101).

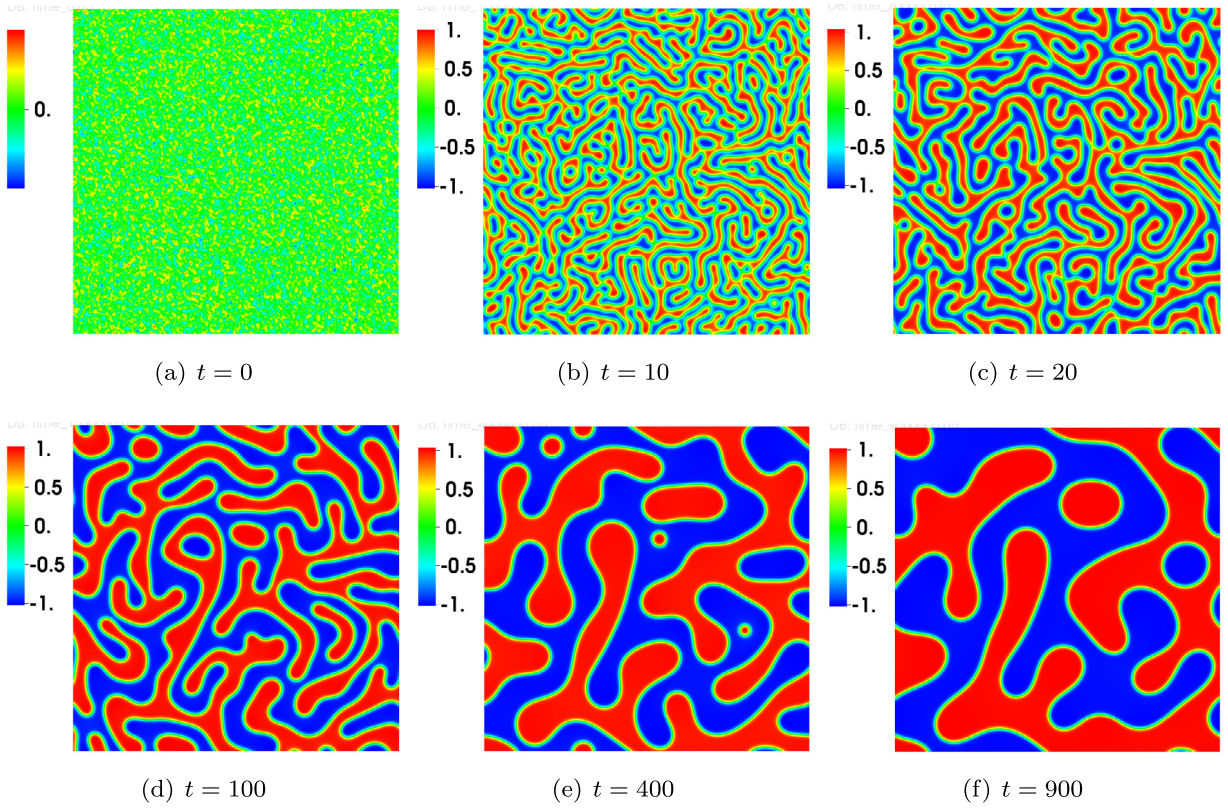

Fig. 3. The isolines of numerical solutions of the ϕ for the Cahn–Hilliard equation using the full discrete scheme. The time step is $\delta t = 0.001$. Snapshots are taken at $t = 0, 10, 20, 100, 400, 900$, respectively.

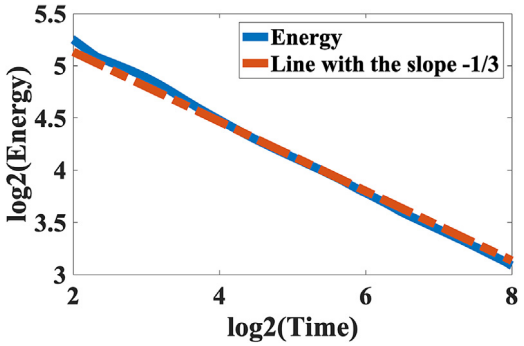

Fig. 4. Free energy evolution of the coarsening dynamics predicted by the Cahn–Hilliard equation. The x-axis and y-axis are in the $\log_2$ scale. It indicates the free energy decays following a power law of $-\frac{1}{3}$, i.e. $E(t) \approx O(t^{-\frac{1}{3}})$. This result agrees well with the report in literature [44].

References

[1] J.W. Cahn, J.E. Hilliard, Free energy of a nonuniform system. I. Interfacial free energy, J. Chem. Phys. 28 (2) (1958) 258–267.
[2] J. Lowengrub, L. Truskinovsky, Quasi-incompressible Cahn-Hilliard fluids and topological transitions, Proc. Math. Phys. Eng. Sci. 454 (1978) (1998) 2617–2654.
[3] L.Q. Chen, J. Shen, Applications of semi-implicit Fourier-spectral method to phase field equations, Commun. Comput. Phys. 108 (2–3) (1998) 147–158.
[4] L.Q. Chen, Phase-field models for microstructure evolution, Ann. Rev. Mater. Res. 32 (1–2) (2002) 113–140.
[5] J.J. Eggleston, G.B. Mcfadden, P.W. Voorhees, A phase field model for highly anisotropic interfacial energy, Phys. D 150 (1–2) (2001) 91–103.
[6] Q. Du, C. Liu, X. Wang, Simulating the deformation of vesicle membranes under elastic bending energy in three dimensions, J. Comput. Phys. 212 (2) (2006) 757–777.
[7] M.G. Forest, Q. Wang, X. Yang, LCP droplet dispersions: a two-phase, diffuse-interface kinetic theory and global droplet defect predictions, Soft Matter 8 (37) (2012) 9642–9660.

[8] C.M. Elliott, A.M. Stuart, The global dynamics of discrete semilinear parabolic equations, SIAM J. Numer. Anal. 30 (6) (1993) 1622–1663.
[9] D. Eyre, Unconditionally gradient stable time marching the Cahn-Hilliard equation, in: Computational and Mathematical Models of Microstructural Evolution (San Francisco, CA, 1998), Vol. 529, MRS, 1998, pp. 39–46.
[10] Z. Hu, S.M. Wise, C. Wang, J.S. Lowengrub., Stable and efficient finite difference nonlinear-multigrid schemes for the phase field crystal equation, J. Comput. Phys. 228 (2009) 5323–5339.
[11] S. Wise, C. Wang, J.S. Lowengrub, An energy-stable and convergent finite-difference scheme for the phase field crystal equation, SIAM J. Numer. Anal. 47 (3) (2009) 2269–2288.
[12] C. Wang, S.M. Wise, An energy stable and convergent finite-difference scheme for the modified phase field crystal equation, SIAM J. Numer. Anal. 49 (2011) 945–969.
[13] J. Shen, C. Wang, X. Wang, S.M. Wise, Second-order convex splitting schemes for gradient flows with ehrlicha-schwoebel type energy: Application to thin film epitaxy, SIAM J. Numer. Anal. 50 (1) (2012) 105–125.
[14] A. Diegel, C. Wang, X. Wang, S. Wise, Convergence analysis and error estimates for a second order accurate finite element method for the Cahn-Hilliard-Navier-Stokes system, Numer. Math. 137 (3) (2017) 495–534.
[15] J. Zhu, L.Q. Chen, J. Shen, V. Tikare, Coarsening kinetics from a variable-mobility Cahn-Hilliard equation: application of a semi-implicit Fourier spectral method, Phys. Rev. E 60 (4) (1999) 3564.
[16] J. Shen, X. Yang, Numerical approximations of Allen-Cahn and Cahn-Hilliard equations, Discrete Contin. Dyn. Syst. 28 (2010) 1669–1691.
[17] R. Chen, G. Ji, X. Yang, H. Zhang, Decoupled energy stable schemes for phase-field vesicle membrane model, J. Comput. Phys. 302 (2015) 509–523.
[18] C. Liu, J. Shen, X. Yang, Dynamics of defect motion in nematic liquid crystal flow: modeling and numerical simulation, Commun. Comput. Phys. 2 (2007) 1184–1198.
[19] C. Xu, T. Tang, Stability analysis of large time-stepping methods for epitaxial growth models, SIAM J. Numer. Anal. 44 (4) (2006) 1759–1779.
[20] X. Yang, M.G. Forest, C. Liu, J. Shen, Shear cell rupture of nematic liquid crystal droplets in viscous fluids, J. Non-Newton. Fluid Mech. 166 (2011) 487–499.
[21] J. Zhao, X. Yang, Y. Gong, Q. Wang, A novel linear second order unconditionally energy stable scheme for a hydrodynamic Q-tensor model of liquid crystals, Comput. Methods Appl. Mech. Engrg. 318 (2017) 803–825.
[22] F. Guillén-González, G. Tierra, On linear schemes for a Cahn-Hilliard diffuse interface model, J. Comput. Phys. 234 (2013) 140–171.
[23] S. Dong, Z. Yang, L. Lin, A family of second-order energy-stable schemes for Cahn-Hilliard type equations, J. Comput. Phys. 383 (2019) 24–54.
[24] J. Kim, K. Kang, J. Lowengrub, Conservative multigrid methods for ternary Cahn-Hilliard systems, Commun. Math. Sci. 2 (2004) 53–77.
[25] Y. Li, J. Kim, N. Wang, An unconditionally energy-stable second-order time-accurate scheme for the Cahn-Hilliard equation on surfaces, Commun. Nonlinear Sci. Numer. Simul. 53 (2017) 213–227.
[26] J. Guo, C. Wang, S. Wise, X. Yue, An H^2 convergence of a second-order convex-splitting, finite difference scheme for the three-dimensional Cahn–Hilliard equation, Commun. Math. Sci. 14 (2) (2015) 489–515.
[27] Y. Gao, X. He, L. Mei, X. Yang, Decoupled, linear, and energy stable finite element method for the Cahn-Hilliard-Navier-Stokes-Darcy phase field model, SIAM J. Sci. Comput. 40 (1) (2018) B110–B137.
[28] F. Lin, X. He, X. Wen, Fast, unconditionally energy stable large time stepping method for a new Allen-Cahn type square phase-field crystal model, Appl. Math. Lett. 98 (2019) 248–255.
[29] K. Cheng, Z. Qiao, C. Wang, A third order exponential time differencing numerical scheme for no-slope-selection epitaxial thin film model with energy stability, J. Sci. Comput. 81 (1) (2019) 154–185.
[30] K. Cheng, W. Feng, C. Wang, S. Wise, An energy stable fourth order finite difference scheme for the Cahn-Hilliard equation, J. Comput. Appl. Math. 362 (2019) 574–595.
[31] J. Shen, J. Xu, J. Yang, The scalar auxiliary variable (SAV) approach for gradient flows, J. Comput. Phys. 353 (2018) 407–416.
[32] D. Li, Z. Qiao, T. Tang, Characterizing the stabilization size for semi-implicit Fourier-spectral method to phase field equations, SIAM J. Numer. Anal. 54 (3) (2016) 1653–1681.
[33] D. Li, Z. Qiao, On second order semi-implicit Fourier spectral methods for 2D Cahn-Hilliard equations, J. Sci. Comput. 70 (1) (2017) 301–341.
[34] S. Badia, F. Guillén-González, J.V. Gutiérrez-Santacreu, Finite element approximation of nematic liquid crystal flows using a saddle-point structure, J. Comput. Phys. 230 (4) (2011) 1686–1706.
[35] X. Yang, J. Zhao, Q. Wang, J. Shen, Numerical approximations for a three components Cahn-Hilliard phase-field model based on the invariant energy quadratization method, Math. Models Methods Appl. Sci. 27 (2017) 1993–2023.
[36] X. Yang, L. Ju, Efficient linear schemes with unconditional energy stability for the phase field elastic bending energy model, Comput. Methods Appl. Mech. Engrg. 315 (2017) 691–712.
[37] X. Yang, J. Zhao, Q. Wang, Numerical approximations for the molecular beam epitaxial growth model based on the invariant energy quadratization method, J. Comput. Phys. 333 (2017) 102–127.
[38] X. Yang, G. Zhang, Numerical approximations of the Cahn-Hilliard and Allen-Cahn equations with general nonlinear potential using the invariant energy quadratization approach, 2017, arXiv:1712.02760v1.
[39] X. Yang, J. Zhao, On linear and unconditionally energy stable algorithms for variable mobility Cahn-Hilliard type equation with logarithmic Flory-Huggins potential, Commun. Comput. Phys. 25 (2019) 703–728.
[40] J. Zhao, X. Yang, Y. Gong, X. Zhao, X.G. Yang, J. Li, Q. Wang, A general strategy for numerical approximations of non-equilibrium models–Part I thermodynamical systems, Int. J. Numer. Anal. Model. 15 (6) (2018) 884–918.
[41] Y. Gong, J. Zhao, Energy-stable Runge–Kutta schemes for gradient flow models using the energy quadratization approach, Appl. Math. Lett. 94 (2019) 224–231.
[42] J. Shen, J. Xu, Convergence and error analysis for the scalar auxiliary variable (SAV) schemes to gradient flows, SIAM J. Numer. Anal. 56 (2018) 2895–2912.
[43] Z. Zhang, Z. Qiao, An adaptive time-stepping strategy for the Cahn-Hilliard equation, Commun. Comput. Phys. 11 (4) (2012) 1261–1278.
[44] S. Dai, Q. Du, Computational studies of coarsening rates for the Cahn-Hilliard equation with phase-dependent diffusion mobility, J. Comput. Phys. 310 (2016) 85–108.